BNNSs-OH/CAB COMPOSITE COATINGS AS A NOVEL FILM FOR HIGHLY EFFICIENT WATER VAPOR BARRIER PROPERTY

SHUAIPENG WANG,[*,**,***] DONGLIN HAN,[*,**,***] YIDI CHAI,[*,**,***] KAI LIU,[*,**,***] KUN LIANG,[*,**,***] XIANQING ZENG,[*,**,***] RONG ZHOU,[*,**,***] LINQING GUO,[*,**,***] YEXIAN CHEN,[*,**,***] NINGNING HOU,[*,**,***] HONGWEI LI[*,**,***] and YUCHUAN HUANG[*,**,***]

[*]*China Tobacco Sichuan Industrial Company Ltd., Chengdu 610094, Sichuan, People's Republic of China*
[**]*New Tobacco Products Engineering and Technology Research Center of Sichuan Province, Chengdu 610094, Sichuan, People's Republic of China*
[***]*Harmful Components and Tar Reduction in Cigarette Key Laboratory of Sichuan Province, Chengdu 610094, Sichuan, People's Republic of China*
✉ *Corresponding author: Y. Huang, wsp0351@163.com*

Received April 1, 2022

Cellulose-based composite packaging films are regarded as environmentally friendly materials due to their complete degradability, as compared with plastic materials. Herein, a high-barrier composite coated paper was fabricated by coating cellulose acetate butyrate (CAB) with different concentrations of edge hydroxylated boron nitride (BNNSs-OH), and then the effects of water vapor barrier, along with composition ratio and film-forming thickness in gradient setting were evaluated. The composite membrane is more likely to create higher barrier performance as the concentration of BNNSs-OH increases. In view of mechanical properties and barrier properties, the best barrier effect is achieved when the hydroxylated boron nitride solution content is 12.5 wt% and the composite thickness is 100 μm, and the water vapor transmission rate is as low as 120.8 g/m^2·day. Paper coated with BNNSs-OH/CAB may be used for packaging, showing promising potential not only for the food sector, but also for other application areas.

Keywords: cellulose acetate butyrate, edge-hydroxylated boron nitride, water vapor barrier

INTRODUCTION

Barrier coating on paper for packaging applications is a versatile and effective method. The packaging materials are conventionally limited to high polymer materials, such as polybutylene adipate terephthalate,[1] polyethylene terephthalate[2] and polyethylene.[3] Considering the depletion of non-renewable resources and environmental pollution, a good deal of requirements are put forward for the selection of packing materials, which are recommended to be biodegradable, widely sourced, and to have remarkable performance. Hence, an increasing number of researchers are focusing on sustainable and renewable alternatives.[4] Cellulose is one of the most abundant biomass materials on the planet and is considered as an ideal substitute to replace non-renewable petroleum polymers theoretically. Cellulose acetate butyrate is processed from cellulose, which is a good choice for polymer coating due to its extraordinary film formation.[6] Packaging materials should prevent the evaporation of water vapor, so that the moisture of the products packaged will not be lost. However, when cellulose is used as packaging, it will absorb water vapor because of its hydrophilicity, resulting in continuous loss of moisture.[7] Therefore, cellulose is not suitable for packaging applications without modification.

In light of that, CAB/polyethylene glycol/aryl ammonium cation modified clay composite films, with outstanding vapor barrier characteristics, have been developed by Nayan Ranjan Saha *et al*.[8] Many studies have explored adding various inorganic fillers to CAB as a foundation to increase barrier performance.[9-11] Additives, including inorganic nanoparticles or nanosheets, were employed to improve water vapor barrier characteristics.[12] Hexagonal boron nitride (h-BN) is a graphite-like material with strong molecular bonding force owing to two-dimensional planes and weak van der Waals bridging between planes. This sort of multilayer provides a tortuous route structure that effectively increases the gas barrier performance of coated paper by preventing water vapor

penetration.[13] The increased aspect ratio of h-BN over clay is the most evident advantage. As the aspect ratio rises, the tortuous path lengthens, and the gas molecules fill the longer path, resulting in a reduction in permeability. However, h-BN is generally difficult to disperse in polymers, especially when it is in the form of an agglomerate. Because of the presence of hydroxyl groups, h-BN can be edge-hydroxylated to improve compatibility with CAB, due to the presence of hydroxyl groups. The ethanol solution can help h-BN to disperse within the CAB matrix. By producing h-BN nanosheets using liquid-phase exfoliation, Muhammad *et al*. created h-BN-polyurethane composites with outstanding CO_2 barrier characteristics.[14]

In this work, the edge-hydroxylated BNNSs (BNNSs-OH) were successfully prepared and scattered in a CAB matrix with ethanol solution. Then, the solution was used for coating base paper to form coated paper in order to study the water vapor barrier properties enhancement and mechanical properties. The composite films maintained good mechanical strength owing to the base paper. The barrier properties of the coated paper were shown to be more dependent on the content of BNNSs-OH, while the mechanical properties were mainly dependent on the base paper. When the hydroxylated boron nitride solution content was 12.5 wt%, the coated paper was found to be the most effective in preventing water vapor from passing through the film, with a WVTR of 120.6 g/m^2•24h, the highest tensile strength (49.4 MPa), and a balance of mechanical and barrier qualities.

EXPERIMENTAL

Materials

Cellulose acetate butyrate (CAB-553-0.4, 46.0 wt% of butyryl, 2.0 wt% of acetyl, and 4.8 wt% of hydroxyl, M_n of 12,000 g mol^{-1}), hexagonal boron nitride (h-BN) with a lateral size of approximately 1 μm, N,N-dimethylformamide (DMF), ethanol (AR, 99.7%), urea and base paper were used in this study. All chemicals mentioned above were of analytical grade and were used without further purification. Water was purified through a Millipore system (>18MΩ) and was then used to prepare solutions.

Preparation of BNNSs-OH

h-BN powder was spread in DMF and ultrasonically treated for 8 hours to get exfoliated BNNS nanosheets, based on prior work by the research group of Wu.[15] Ball milling using BNNSs/urea/deionized water (1:60:30 by weight) at 800 rpm for 15 hours yielded edge-hydroxylated boron nitride (BNNSs-OH). The suspension was then rinsed with deionized water to remove any remaining urea, then centrifuged for 15 minutes at 3000 rpm to remove the bottom sediment. Finally, the BNNSs-OH powder was produced, following vacuum filtering and 3 hours of drying in an 80 °C vacuum oven.

Preparation of composite film

In this work, BNNSs-OH power was slowly added into ethanol absolute for 20 minutes and stirred intensely at 1500 rpm. Then, CAB was added into the above suspension under intense stirring at 1500 rpm to obtain a mixed slurry. After removing the air bubbles under vacuum conditions, the mixed slurry was applied as a coating on the paper, using a scraper, in a thickness of 100 μm. Generally speaking, the thicker the coating, the better the barrier effect.

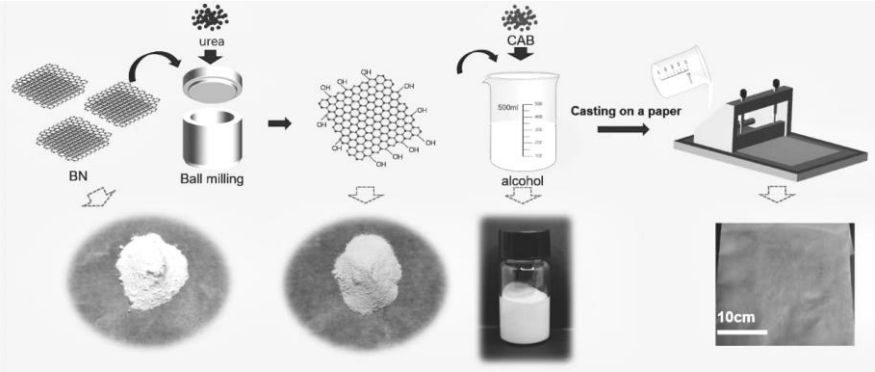

Figure 1: Schematic diagram of composite film fabrication

The weight ratios between CAB and BNNSs-OH were 2.5/97.5, 5/95, 7.5/92.5, 10/90, and 12.5/87.5, respectively. Then, the coated papers were called as BNNS-2.5, BNNS-5, BNNS-7.5, BNNS-10 and BNNS-12.5, correspondingly. For comparison, the CAB solution without BNNSs-OH added and h-BN (12.5 wt%) were called P-CAB and BN-12.5, respectively.

Characterizations

The surface and cross-section of the samples were observed by scanning electron microscopy (SEM, NOVA NANOSEM 450), at an accelerating voltage of 5 kV. The morphologies of BNNS-OH/CAB were acquired by a transmission electron microscope (TEM, JEF-2100F, JEOL) and the thickness of the BNNS-OH/CAB was measured by atomic force microscopy (AFM, 359 Marin Keys Blvd, Suite 20, USA). Thermogravimetric analysis (TGA Q500, TA, USA) was carried out to analyze the thermal stability of coated papers. The effectiveness of the edge-hydroxylation process and the formation of BNNSs-OH were indicated by X-ray photoelectron spectroscopy (XPS, Axis Ultra DLD, UK). X-ray photoelectron spectroscopy (XRD, Ultima IV diffractometer, Rigaku, Japan) was used to probe BNNSs-OH and composite films with a scanning speed of 4 °C min^{-1} in the range from 2 to 70° (40 kV and 40 mA). Fourier transform infrared spectroscopy (FTIR) was carried out on a Bruker Tensor 27 spectrometer in the wavenumber range of 4000–400 cm^{-1}. The tensile strength (σ_b) and strain (ε) values of the composites were characterized by FAVIGRAPH semiautomatic equipment (Textechno Company, Germany) at room temperature with a cross-head speed of 20 mm min^{-1}.[16] Water vapor transmission rate (WVTR) was used to verify the moisture resistance for the composite coated paper using a Mocon Permatran® W3/31 (Modern Controls Inc.), in compliance with ASTM F1249-90 (37.8 °C and 90% relative humidity). Briefly, the sample, of about 100 mm in diameter, was prepared and mounted on the mouth of a cylindrical cup containing distilled water. The reported results in [g/m^2•24h] were obtained from at least 3 independent specimens.[17]

confirm whether the edge-hydroxylation was successfully performed or not, the subsequent product was examined by XPS

RESULTS AND DISCUSSION

Morphology of the BNNSs-OH

Because of its considerable thickness, h-BN exhibits low dispersibility in polymer solutions.[18] As shown in Figure 2a, h-BN has a thick sheet form of about 1 μm. As illustrated in Figure 2b, the h-BN was exfoliated under vigorous sonication to separate BNNSs, while the exfoliated BNNSs gained through sonication are very thin and transparent.[19] Fast Fourier transform of AFM images reveals a special six-fold symmetry, indicating that BNNSs have an excellent hexagonal crystalline structure, which we can be seen in Figure 2c. The height information from the AFM image further shows that the thickness of BNNSs-OH is ~6 nm,[20] as shown in Figure 2d. As a result, it appears that BNNSs have been effectively exfoliated and prepared for the subsequent further hydroxylation treatment.

For forming more hydroxyl groups, BNNSs were transformed to BNNSs-OH by ball-milling and urea treatments. To confirm whether the edge-hydroxylation was successfully performed or not, the subsequent product was examined by XPS and XRD. XPS was used for further analyzing the chemical compositions of the BNNSs and BNNSs-OH, as shown in Figure 3a and b. In Figure 3a, it can be found that the B1s core-level spectral images of BNNSs and BNNSs-OH both clearly show separate B-N peaks at 190.3 eV.[21] However, only BNNSs-OH exhibits a faint peak at ~191.1 eV, which indicates B-O (Fig. 3b), indicating that the O atom has been covalently bonded with the positively charged B atom of BNNSs, which was most likely to be the OH group after urea-based ball milling treatment. Furthermore, the BNNSs and BNNSs-OH contain two identical crystal peaks at 25.6^o and 54.2^o in XRD patterns, implying the in-plane orientation of crystal planes (002) and (004).[22] The results above indicate that the hydroxylation process has little effect on the in-plane (surface) crystal structure, and the hydroxyl groups can only be grafted on the edges of BN nanosheets.

In order to compare the dispersion stability of BNNSs and BNNSs-OH in ethanol solution intuitively, each was dispersed into ethanol for 30 minutes using a probe-sonicator (100 W). After standing for 7 days, BNNSs tend to agglomerate and precipitate, but BNNSs-OH still retained some stability and good dispersion in the ethanol solution (Fig. 3d). As a result, it is demonstrated that immediately exposing BNNSs to urea chemical treatment and ball milling at the same time can provide high-quality edge-hydroxylation BNNSs-OH, with the hydroxylation process ensuring the integrity of the crystal structure. Thus, it proves that ball milling for BNNSs with urea results in high-quality edge-hydroxylation BNNSs-OH, which ensures crystal structure integrity due to the

hydroxylation process. Thermogravimetric analysis (TGA) was used to calculate the content of functional groups on BNNSs-OH (Fig. 4). A weight loss of about 2.2% was observed when it was heated from 25 °C to 800 °C. In summary, all these show that edge-hydroxylated BNNSs have been successfully prepared.

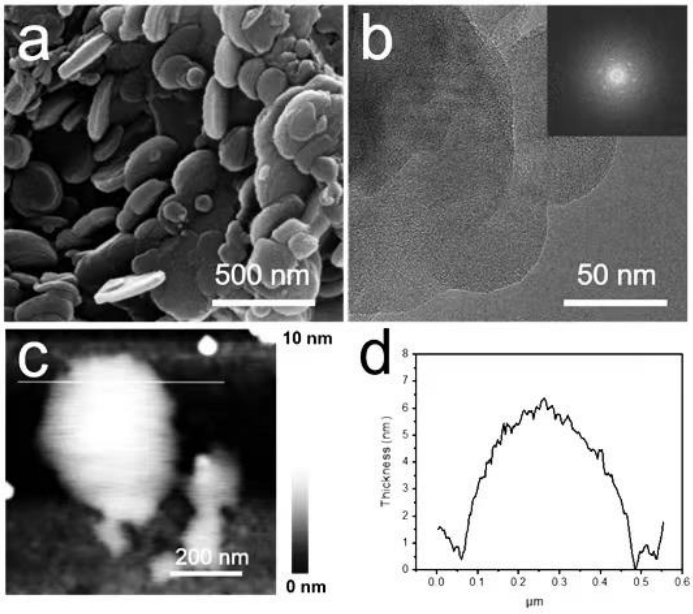

Figure 2: (a) SEM image of h-BN; (b) TEM image of BNNS; (c) AFM image of BNNSs and (d) corresponding height information of BNNSs-OH

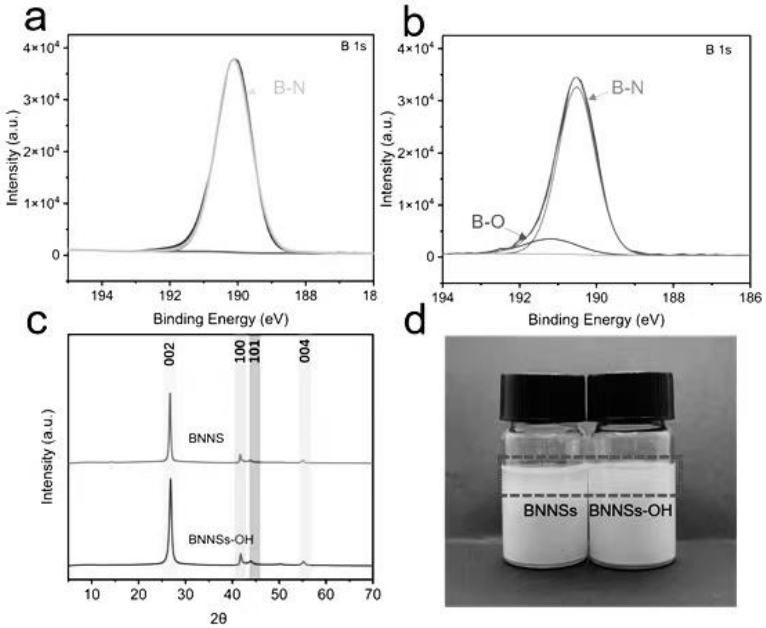

Figure 3: (a,b) XPS B1s of BNNSs and BNNSs-OH, respectively; (c) XRD patterns of BNNSs and BNNSs-OH; (d) Photograph of dispersion of BNNSs and BNNSs-OH in ethanol suspension

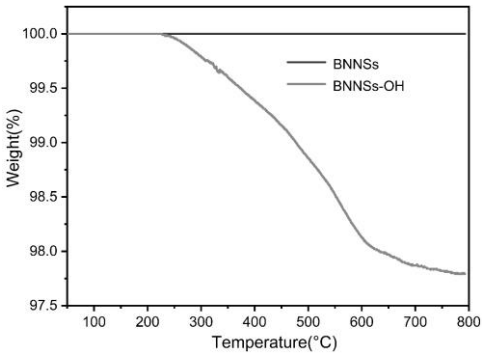

Figure 4: TGA curves of BNNSs-OH and BNNSs

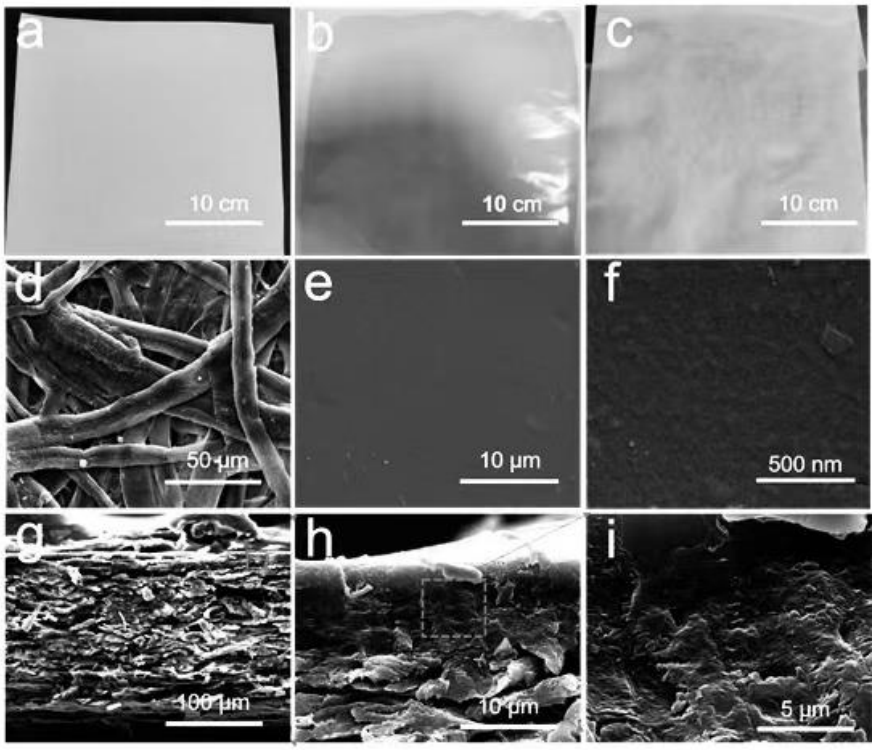

Figure 5: (a-c) Photographs of paper, P-CAB film and BNNS-CAB-P film, respectively; (d-f) Surface SEM images of paper, P-CAB film and BNNS-CAB-P film; (g-i) SEM images of the BNNS-CAB-P film

Morphology and structure of composite films

The appearance of the coated paper could be seen through the optical diagram. The reflecting gloss could be detected when CAB was used to coat the base paper, but the reflecting gloss of the sample became dim in the case of the sample coated with BNNSs-OH, as shown in Figure 5a-c, implying that the introduction of BNNSs-OH can impact the surface. SEM was used to examine the surface and cross-section morphology of membranes. Cellulose fiber threads interlaced together on the surface of the paper, resulting in a rough and porous structure (Fig. 5d and g). The upper layer of the lamination is smooth and thick when just CAB was applied to the paper. As can be seen in Fig. 5e and h, the CAB solution filled in the grooves on the base paper surface. The coating is deeply embedded in the paper, with almost imperceptible interface differences, as can be seen in the cross-section (Fig. 5h). The surface of the produced film became uneven, when the BNNSs-OH was added to the CAB solution (Fig. 5f). Also, thanks to the hydroxylation modification, the BNNSs-OH was uniformly dispersed throughout the CAB (Fig. 5i).

Thermogravimetric analysis (TGA) was applied to gauge the thermal stability of coated paper (Fig. 6). All the samples displayed a one-step decomposition under N_2 atmosphere in a stage from 300 to 330 °C, which was attributed to paper depolymerization. Due to the low coating content, the thermal stability of the coated paper film was dominated by that of the paper. To verify whether BNNSs-OH

was successfully added to the composite film, XRD was used to characterize it (Fig. 7). Pure cellulose paper contained three typical characteristic peaks, the 16.2° ($1\bar{1}0$) crystal face peak and the 22.4° (110) crystal face peak. There were two peaks at 25.6° and 54.2°, which were the peaks of BNNSs-OH. For the composite film, the XRD curve had two typical peaks of paper, as well as a peak characteristic of BNNSs-OH. The peak at 54.2° indicated that we compounded CAB and BNNSs-OH together successfully.

Mechanical properties

The stress-strain performance of paper coated with various contents of BNNSs-OH/CAB-P was evaluated, as shown in Figure 8a and b. The tenacity of paper coated with CAB only firstly increases from 45.7 MPa, peaking at 49.4 MPa, and then decreased to 39.9 MPa. The hydroxylated edges may efficiently link the hydroxyl groups with CAB when a tiny quantity of BNNSs-OH is introduced to CAB, somewhat improving the mechanical strength. The mechanical characteristics of the coated papers had little differences in all the samples, which was because the mechanical strength of these samples was given by the paper instead of the coatings. The elongation at break of the coated papers was between 3.02 and 3.42%, indicating that neither the addition of BNNSs-OH/CAB nor the coating application techniques affected the elongation of coated paper.[23] When the concentration reached 12.5 wt% for BNNSs-OH, with the increase in the concentration of BNNSs-OH, there was a negative effect on the mechanical strength, so the maximum proportion of BNNSs-OH should not exceed 12.5 wt%.

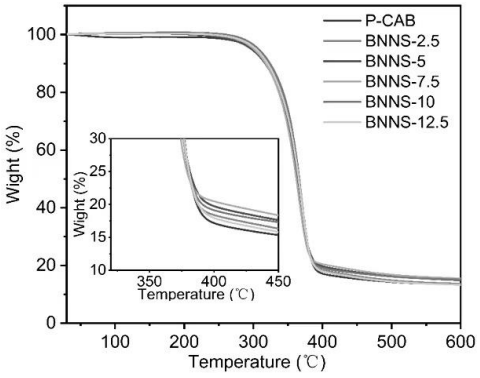

Figure 6: TGA curves of composite films

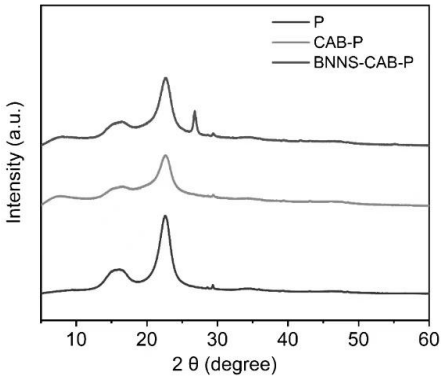

Figure 7: XRD spectra of paper, P-CAB film and BNNS-CAB-P film

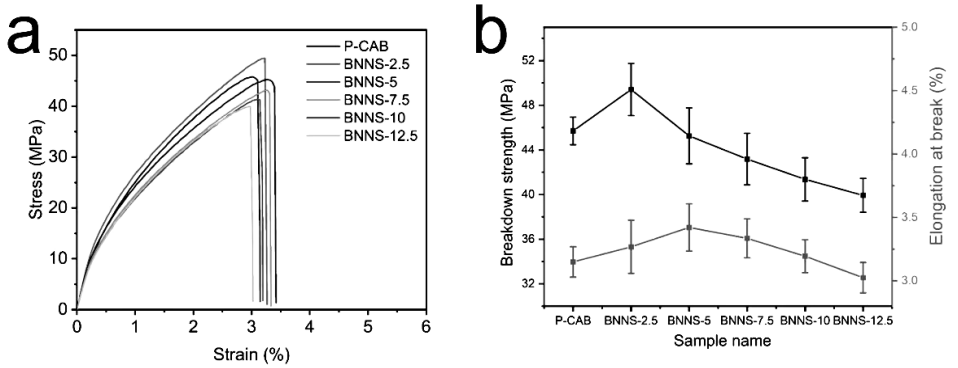

Figure 8: (a) Tensile strength of papers coated with CAB and different concentrations of BNNSs-OH; (b) Elongtion at break of paper coated with CAB and different concentrations of BNNSs-OH

Water vapor barrier properties of coated paper

We measured water vapor barrier chracteristics in terms of WVTR to see how varying BNNSs-OH concentrations affected the coated paper's water vapor barrier capabilities (Fig. 9). As the BNNSs-OH content of the coated sheets increased, the WVTR decreased from 296.6 g/m^2·24h to 120.8 g/m^2·24h, as shown in Figure 9. As the ethanol solution evaporates, BNNSs-OH will spread flat on the surface of the coated paper. There are more tortuous paths when forcing water vapor molecules to diffuse through the lamellae parallel to the surface.[24] Due to poor dispersity in CAB, the barrier performance of

BNNSs without edge-hydroxylation treatment is only 168.6 g/m^2·24h at the same 12.5% content. The coated paper-packed BNNSs-OH layer with 12.5 wt% could better prevent the water vapor from passing through the film, resulting in decreased water vapor permeability in the longitudinal direction.[25] Thus, BNNSs-OH coating for a stacked layered structure endows superior barrier performance to the coated paper.

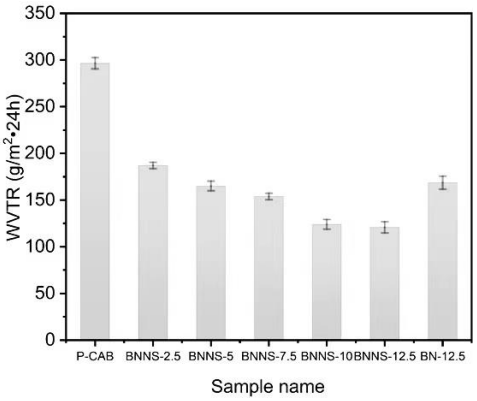

Figure 9: Water vapor transmission rates (WVTR) of coated papers

CONCLUSION

BN nanosheets were edge-hydroxylated in this study to improve their dispersibility in an ethanol solution. By enhancing the dispersion of two-dimensional inorganic fillers, the barrier properties of the composite film could be improved and the content of the filler was reduced. With a balance of mechanical and barrier qualities, the coated paper-packed BNNSs-OH layer with 12.5 wt% was able to better prevent water vapor from flowing through the film, with a WVTR of 120.8 g/m^2·24h and maximum tensile strength of 49.4 MPa. The concentration of BNNSs-OH was found to have a greater impact on the coated paper's barrier qualities, while the mechanical properties were largely determined by the base paper. More importantly, as a renewable and biodegradable materials, CAB and paper might partially replace petrochemical-based packaging. In the realm of food packaging, BNNSs-OH/CAB composite coated papers offer the possibility of water vapor barrier and mechanical damage protection.

ACKNOWLEDGMENTS: This work was financially supported by the Special Project of the State Tobacco Monopoly Administration (Grant No. 1102021001021). The authors thank New Tobacco Products Engineering and Technology Research Center of Sichuan Province (Grant No. JL/SCZYG SJ001-03).

REFERENCES

[1] W. Katekhong, P. Wongphan, P. Klinmalai and N. Harnkarnsujarit, *Food Chem.*, **374**, 131709 (2022), https://doi.org/10.1016/j.foodchem.2021.131709

[2] L. Yin and Q. Chen, *Mater. Sci. Eng.*, **274**, 012042 (2017), https://doi.org/10.1088/1757-899x/274/1/012042

[3] K. Möller, T. Gevert and A. Holmström, *Polym. Degrad. Stab.*, **73**, 69 (2001), https://doi.org/10.1016/S0141-3910(01)00067-2

[4] B. Nitya, S. V. Singh, R. S. Mor and K. Kshitiz, *Trends Food Sci. Technol.*, **105**, 385 (2020), https://doi.org/10.1016/j.tifs.2020.09.015

[5] D. Klemm, B. Heublein, H. P. Fink and A. Bohn, *Angew. Chem. Int. Ed.*, **44**, 22 (2005), https://doi.org/10.1002/anie.200460587

[6] C. J. Malm, O. W. Kaul and G. D. Hiatt, *J. Ind. Eng. Chem.*, **43**, 1094 (2002), https://doi.org/10.1021/ie50497a028

[7] H. Zhu, W. Luo, P. N. Ciesielski, Z. Fang, J. Y. Zhu *et al.*, *Chem. Rev.*, **116**, 16 (2016), https://doi.org/10.1021/acs.chemrev.6b00225

[8] N. R. Saha, I. Roy, G. Sarkar, A. Bhattacharyya, R. Das *et al.*, *Carbohyd. Polym.*, **187**, 8 (2018), https://doi.org/10.1016/j.carbpol.2018.01.065

[9] C. C. Pola, E. A. A. Medeiros, O. L. Pereira, V. G. L. Souza, C. G. Otoni *et al.*, *Food Packag. Shelf Life*, **9**, 69 (2016), https://doi.org/10.1016/j.fpsl.2016.07.001

[10] R. I. Quintero, M. J. Galotto, F. Rodriguez and A. Guarda, *Packag. Technol. Sci.*, **27**, 6 (2014),

https://doi.org/10.1002/pts.2043
[11] H. Ferfera-Harrar and N. Dairi, *Iran*. *Polym*. *J*., **23**, 12 (2014), https://doi.org/10.1007/s13726-014-0286-z
[12] H. A. El-Rehim, H. Kamal, E.-S. A. Hegazy, E.-S. Soliman and A. Sayed, *Radiat*. *Phys*. *Chem*., **153**, 180 (2018), https://doi.org/10.1016/j.radphyschem.2018.08.007
[13] G. C. Pradhan, L. Behera and S. K. Swain, *Chin*. *J*. *Polym*. *Sci*., **32**, 10 (2014), https://doi.org/10.1007/s10118-014-1511-0
[14] M. Azeem, R. Jan, S. Farrukh and A. Hussain, *Results Phys*., **12**, 1535 (2019), https://doi.org/10.1016/j.rinp.2019.01.057
[15] K. Wu, J. Fang, J. Ma, R. Huang, S. Chai *et al*., *ACS Appl*. *Mater*. *Interfaces*, **9**, 35 (2017), https://doi.org/10.1021/acsami.7b08214
[16] D. Mondal, M. M. R. Mollick, B. Bhowmick, D. Maity, M. K. Bain *et al*., *Prog*. *Nat*. *Sci*., **23**, 6 (2013), https://doi.org/10.1016/j.pnsc.2013.11.009
[17] D. Mondal, B. Bhowmick, M. M. Mollick, D. Maity, A. Mukhopadhyay *et al*., *Carbohyd*. *Polym*., **96**, 1 (2013), https://doi.org/10.1016/j.carbpol.2013.03.064
[18] K. Wu, P. Liao, R. Du, Q. Zhang, F. Chen *et al*., *J*. *Mater*. *Chem*. *A*, **6**, 25 (2018), https://doi.org/10.1039/c8ta03642j
[19] U. Khan, A. O'Neill, M. Lotya, S. De and J. N. Coleman, *Small*, **6**, 7 (2010), https://doi.org/10.1002/smll.200902066
[20] K. K. Kim, A. Hsu, X. Jia, S. M. Kim, Y. Shi *et al*., *Nano Lett*., **12**, 1 (2012), https://doi.org/10.1021/nl203249a
[21] Q. Liu, C. Chen, M. Du, Y. Wu, C. Ren *et al*., *ACS Appl*. *Nano Mater*., **1**, 9 (2018), https://doi.org/10.1021/acsanm.8b00867
[22] C. Lei, K. Wu, L. Wu, W. Liu and R. Du, *J*. *Mater*. *Chem*. *A*, **7**, 33 (2019), https://doi.org/10.1039/C9TA05067A
[23] W. Brostow and D. Zhang, *Mater*. *Lett*., **276**, 128179 (2020), https://doi.org/10.1016/j.matlet.2020.128179
[24] L. E. Nielsen, *J*. *Macromol*. *Sci*. *A*, **1**, 5 (1967), https://doi.org/10.1080/10601326708053745
[25] G. L. Graff, R. E. Williford and P. E. Burrows, *J*. *Appl*. *Phys*., **96**, 4 (2004), https://doi.org/10.1063/1.1768610